28th AIAA Applied Aerodynamics Conference
28 June - 1 July 2010, Chicago, Illinois

AIAA 2010-4675

Aerodynamic Shape Optimization of Fan-Flow Deflectors for Noise Reduction Using Adjoint Method

Juntao Xiong *, Feng Liu † and Dimitri Papamoschou ‡

University of California Irvine, Irvine, CA, 92697-3975, USA

This article presents application of an adjoint method to the aerodynamic shape optimization of deflector vanes installed in the fan nozzle of a turbofan engine. The purpose of the vanes is to reduce jet noise radiated towards the community, and the specific application of this study is for a supersonic turbofan engines with bypass ratio 2.7. The cost function used in the optimization includes entropy generation and a penalty for deviating from a target deflection angle. The initial vane airfoil is the NACA0012. The vane airfoil arising from the optimization produces flat distributions of pressure coefficient over the surface of the vane thus preventing the formation of sonic bubble and strong shocks. For a fixed flow deflection angle, the optimal airfoil is up to 22.5% more efficient in terms of specific thrust loss compared to the NACA0012. Importantly, the optimization leads to a thicker airfoil with 15% thickness which may be advantageous for structural reasons.

Nomenclature

c	=	vane chord length
C_p	=	pressure coefficient
D_f	=	nozzle fan diameter
$\mathbf{K}_{ij}$	=	Transformation functions between the physical and computation domain
I	=	cost function
M	=	Mach number
NPR	=	nozzle pressure ratio
N_i	=	Unit normal vector in the physical domain, pointing outward from the flow field
p	=	static pressure
q	=	dynamic pressure
R	=	flow equation
s	=	Entropy per unit mass
s_{gen}	=	Entropy generation rate
$\mathcal{T}$	=	thrust
$\mathcal{T}_s$	=	specific thrust
W	=	conservative variable vector
x, y, z	=	Cartesian coordinates
α	=	angle of attack, closure coefficient
ϵ	=	plume deflection angle
Λ	=	weight of penalty function
Ψ	=	co-state variables

*Post-doctoral Researcher, Department of Mechanical Aerospace Engineering, Member AIAA
†Professor, Department of Mechanical and Aerospace Engineering, Associate Fellow AIAA
‡Professor, Department of Mechanical and Aerospace Engineering, Fellow AIAA

I. Introduction

The idea of tilting the bypass stream with fan flow deflectors of a turbofan engine to reduce jet noise was proposed by Papamoschou.[1,2] Figure 1 depicts the general concept. Airfoil-shaped vanes are installed inside the fan duct, in the proximity of the fan exit plane, and deflect the fan flow downward. The overarching principle of the concept is the reduction of the convective Mach number of the turbulent eddies generated by the high speed hot core flow. Mean flow surveys show that the misalignment of the fan and core flows causes a thick, low-speed secondary core on the underside of the high-speed primary flow, especially in the region near the end of the primary potential core, which contains the strongest noise sources. The secondary core reduce the convective Mach number of the primary eddies, thus hindering their ability to generate sound that travels to the downward far field. Past subscale experiments have demonstrated significant reductions in perceived noise level.[3,4]

As with any noise reduction scheme, it is important to assess and mitigate the aerodynamic penalty. Past experiments utilized vanes with classical airfoil geometries (NACA0012, NACA4412, and NACA7514). These airfoils were designed for uniform freestream environment, which is much different than the accelerating freestream present around the internal deflector vanes. Previous computational results[5] revealed that the symmetric NACA0012 has a tendency of generating excessive suction near the leading edge, while the cambered NACA4412 and NACA7514 produce a large supersonic pocket over the airfoil resulting in the formation of a strong shock wave. These underdesirable characteristics of the classical airfoil motivated the design for an optimum vane shape for the noise-suppressing deflector applications.

The aerodynamic shape optimization of the deflector vanes is performed using an adjoint approach is advocated by Jameson,[6] who initially used it for the optimization of two-dimensional airfoil, then for wings and eventually for entire aircraft configurations[7,8] At present, the adjoint method is widely used in optimization problems since it eliminates the explicit dependence of gradient information on the variation of the flow field, through the use of the adjoint equations to the original flow equations. The complete gradient information needed for optimization can be obtained by solving the governing flow equations and the corresponding adjoint equations only once, regardless of the number of design parameters.

In this study the fan nozzle with only a single pair of deflector vanes mounted at 90° azimuth angle is used as design configuration and NACA0012 airfoil profile is used as base reference. The adjoint program is developed based on the PARCAE code which is multi-block parallel flow solver.[5] The cost function is defined as the sum of entropy generation per unit mass flow rate with penalty function. The article outlines how the adjoint equations are derived from the flow equations and how the optimization algorithm is used to design the fan flow deflector vane shape in an accelerating flow.

II. Adjoint Approach

II.A. Design Objectives

The dual-stream nozzle used in this optimization study is based on a scaled-down version of the 3BB nozzle[9] used for noise reduction research at the NASA Glenn Research Center. The fan duct was reduced in diameter to produce BPR=2.7 at the takeoff exhaust conditions. Relevant to this study is the fan operating condition NPR=2.25 resulting in a perfectly expanded Mach number of 1.15. The fan exit diameter is $D_f = 28.1$ mm and the exit height is 1.8 mm. The Reynolds number based on fan exit height is 0.92×10^6. The nozzle coordinates are shown in Figure 2. In this study the fan nozzle with one pair of deflector vanes mounted at 90° azimuth angle is used as design configuration. The vane trailing edge is situated at 2 mm (1.1 fan exit heights) upstream of the nozzle exit. Figure 3(a) shows the nozzle and vane configuration.

The optimization objective is to minimize the aerodynamic penalties of fan flow deflector vanes. The cost function comprises the entropy generation caused by the vanes and a penalty for deviating from a target flow deflection angle.

$$I = s_{gen} + \Lambda|\bar{\beta} - \bar{\beta}_0| \tag{1}$$

where s_{gen} is the mass-averaged entropy generation,

$$s_{gen} = \frac{\int_{B_e} \rho u_j s N_j dA}{\int_{B_e} \rho u_j N_j dA} \tag{2}$$

and $\bar{\beta}$ is the mass-averaged flow deflection angle

$$\bar{\beta} = \frac{\int_{B_e} \rho u_j \beta N_j dA}{\int_{B_e} \rho u_j N_j dA} \tag{3}$$

β is the flow deflection angle on each cell face at exit surface and is defined as the ratio of vertical velocity to axial velocity. B_e is the nozzle exit surface, $\bar{\beta}_0$ is the initial mass-averaged exit flow deflection angle, and Λ is the weight of penalty function. In this study the Hicks-Henne shape functions[10] are adopted as design parameters to modify the upper surface of the deflector vanes. The lower surface is identically modified to fulfill the requirement of a symmetric section.

II.B. Adjoint Equation

As detailed in Jameson's paper,[8] the variation of cost function consists of two terms, one due to variation of flow field and the other due to modification in boundaries. The variation of the flow field δW depends implicitly on the variation of the geometry $\delta\mathcal{F}$ through the Navier-Stokes equations. We multiply the flow equations by a Lagrange multiplier Ψ^T, adding it to the variation of cost function and then eliminating the explicit dependence of δI on δW by setting

$$\left[\frac{\partial I}{\partial W}\right]^T - \left[\frac{\partial R}{\partial W}\right]^T = 0 \tag{4}$$

which is recognized as the adjoint equation, we have

$$\delta I = G\delta\mathcal{F} \tag{5}$$

where G is the gradient

$$G = \left[\frac{\partial I}{\partial \mathcal{F}}\right] - \Psi^T \left[\frac{\partial R}{\partial \mathcal{F}}\right] \tag{6}$$

The optimization problem is then reduced to solving the governing flow equations and their corresponding adjoint equations to obtain the value of Ψ. The gradient can be easily and efficiently computed even for large number of design parameters because the computation cost only depends on the perturbation of geometry.

In this study, the cost function is defined as an integral over the fan nozzle exit surface (Eqn. 1). A weak form of the Navier-Stokes equations is

$$\int_D \frac{\partial \Psi^T}{\partial \xi_i}(\delta F_i - \delta F_{vi})dD - \int_B \Psi^T(\delta F_i - \delta F_{vi})dB = 0 \tag{7}$$

where $F_i = S_{ij}f_j$, $F_{vi} = S_{ij}f_{vj}$, and $S_{ij} = JK_{ij}^{-1}$, $K_{ij} = \frac{\partial x_i}{\partial \xi_j}$. Adding Eqn.(7) to the variation of cost function, we have

$$\begin{aligned} \delta I &= \int_{B_e} \delta C dB - \int_B n_i \Psi^T(\delta F_i - \delta F_{vi})dB \\ &+ \int_D \frac{\partial \Psi^T}{\partial \xi_i}(\delta F_i - \delta F_{vi})dD \end{aligned} \tag{8}$$

where C is a scalar function of both flow variables and geometric variables and depends on the definition of cost function.

The term δC is divided into two terms, δC_f which denotes the flow variation term, and δC_g which denotes the geometry variation term. δC_f can be used to determine the boundary conditions for viscous adjoint equations and thus be eliminated in the cost function. Finally, the variation of cost function can be written in a simplified form:

$$\begin{aligned} \delta I &= \int_{B_{IEF}} [-n_i(\delta S_{ij})\Psi^T f_j + \delta C_g]dB \\ &+ \int_{B_W} [n_i(\delta S_{ij})\psi_k(\sigma_{jk} - p\delta_{jk}) + \delta C_g]dB \\ &+ \delta I_g \end{aligned} \tag{9}$$

where δC_g denotes the variation of cost function due to geometry variation. The subscript IEF denotes the inlet, exit and far field boundaries, and W denotes the wall boundary. The detail adjoint equations and gradient formula can be found in Ref. 10

II.C. Computational Method

Since the properties of the adjoint equations are very similar to the flow equations, the adjoint equations are solved using the same numerical method for flow equations. All the equations are discretized in space by a structured hexahedral grid using a cell-centered finite-volume method. Each grid block is considered as a single entity, only the flow and adjoint quantities at the block boundaries are exchanged. The governing equations are solved explicitly in a coupled manner through a five stage Runge-Kutta scheme towards the steady state with local-time stepping, residual smoothing, and multigrid for convergence acceleration. Further details of the numerical method can be found in Ref. 11

III. Results and Discussion

As mentioned before the fan nozzle with only a single pair of deflector vanes mounted at 90° azimuth angle is used as design configuration in this study. Because all the vane configurations are symmetric to the meridional plane, only one half (180°) of the nozzle was modeled to save computation cost. Multiblock grids are generated for the vane configuration. A C-grid surrounds the vane in the region near the exit plane to capture the features of boundary layer and wake flows accurately. Figure 3(b) shows the computational mesh. Optimization studies are conducted for vane chord lengths of 3 mm and 4 mm. The NACA0012 airfoil is used as the reference vane profile. Based on the gradient obtained from the flow equations and the corresponding adjoint equations, the steepest descent method is chosen as the optimization algorithm to get the desired optimum vane shape.

III.A. Design Point Determination

Previous computational results[5,12] revealed general correlations between the flow losses, deflection angle, and turbulent kinetic energy (TKE) reduction. The larger deflection angle has more effect of reducing downward TKE, which is correlated to the larger reduction of downward radiated noise. On the other hand, higher flow deflection angle is associated with higher thrust loss. Therefore, a balanced choice of the deflection angle must be made. In this study, the mounting azimuthal angle and trailing edge position the of deflector vanes are fixed. We vary the vane chord length and angle of attack to determine the best initial point for the adjoint optimization.

In the discussion that follows, the pressure coefficient is defined as

$$C_p = \frac{p - p_{\mathrm{LE}}}{q_{\mathrm{LE}}}, \tag{10}$$

Where p_{LE} and q_{LE} are the area-averaged pressure and dynamic pressure in the plane of the vane leading edge in the absence of the vane. The nozzle thrust is obtained by integration of the axial momentum and pressure on the exit surface of the fan nozzle.

$$\mathcal{T} = \int_A (\rho u^2 + p - p_a) dA \tag{11}$$

while the specific thrust is

$$\mathcal{T}_s = \frac{\mathcal{T}}{\dot{m}} \tag{12}$$

The overall lift of the nozzle is obtained by integration of the transverse momentum flux on the fan nozzle exit surface.

$$\mathcal{L} = \int_A \rho v u dA \tag{13}$$

and, assuming small angles, the overall deflection of the plume is

$$\epsilon = \frac{\mathcal{L}}{\mathcal{T}} \tag{14}$$

The thrust and specific-thrust losses are defined respectively as

$$\Delta\mathcal{T} = \mathcal{T} - \mathcal{T}_{\text{clean}} \tag{15}$$

$$\Delta\mathcal{T}_s = \mathcal{T}_s - \mathcal{T}_{s,\text{clean}} \tag{16}$$

where the subscript "clean" refers to the clean nozzle without vanes.

Figures 4-5 show the 3-mm and 4-mm chord vane pressure distribution on the midplane of the vane for five angles of attack. The x axes are normalized by the chord length. The C_p^* line marks the critical pressure coefficient where the flow becomes sonic. As the angle of attack increases, the surface pressure distribution develops a sharp suction peak at the leading edge of the airfoil followed by strong pressure rise which thickens the boundary layer. The suction peak causes a supersonic pocket with a possible shock wave at higher angle of attack. Figure 6 shows the relation between the flow deflection angle and the thrust loss. The longer 4-mm chord vane gives better overall performance than the shorter 3-mm chord vane. The losses are very low when the deflection angle is small but they increase rapidly when the deflection angle exceeds about 1.0°. Based on past experience with this nozzle, deflection angles around 1.4° are sufficient to produce significant noise reduction. The corresponding vane angle of attack is about 10°. The deflection angle corresponding to angle of attack 10.0° is deemed to represent the most balanced configuration and is used as a design point for the adjoint optimization method.

III.B. Vane Airfoil Optimization

We begin with optimization results for the 3-mm chord vane. Figure 7 shows the comparison of airfoil shape and surface pressure distributions. The design vane has larger leading edge radius and maximum thickness. The rounder leading edge helps maintain a favorable pressure gradient over the upper surface of the vane. As a result the design vane has a nearly constant pressure over the majority of the upper surface with the pressure bubble at the leading edge completely removed. The reduction in the adverse pressure gradient compared to the NACA0012 vane mitigates the possibility of a shock wave developing. Figure 8 compare Mach number contours between the NACA0012 vane and the design vane. Figures 8(c) and 8(d) depict Mach number contours near the vane leading edge. For the NACA0012 vane we observe a supersonic bubble near the leading edge, with peak Mach number of 1.1. The supersonic bubble followed by a sudden pressure drop which thickens the boundary layer. For the design vane, the Mach number on the upper surface remains nearly constant and the supersonic bubble is completely removed. The maximum Mach number near the leading edge is only 0.9. The near-constant pressure distribution on the upper surface causes the thinner boundary layer. It is notable that the thickness-to-chord ratio of the design vane is 15%. The skin-friction losses from the larger wetted area are negligible compared to the benefits of the more benign pressure distribution. The optimization process resulted in a reduction of thrust loss from 0.162% to 0.145% (10.5% improvement) and a reduction of specific thrust loss from 0.129% to 0.113% (12.4% improvement).

Corresponding results for the 4-mm vane are shown in Figs. 9 - 10. Since the leading edge of the 4-mm vane extends further upstream into a region of low Mach number and low dynamic pressure, the suction peak is much weaker and the pressure bubble is smaller at the leading edge. The maximum Mach number at leading edge is 0.9. The weak suction peak alleviates the possible supersonic pocket with a shock wave and induced separation at higher angle of attack. So the longer vane has an overall better performance than short vane, which reduces the space for design optimization. The optimization trend is still similar to the 3-mm vane, resulting in a thicker airfoil with larger leading edge radius and nearly constant pressure over the majority of the upper surface. The pressure bubble at the leading is completely removed. Again this results in a thinner boundary layer on the vanes surface. The Mach number on the upper surface of the design vane remains nearly constant and the maximum Mach number near the leading edge is 0.7. For the design vanes the thrust loss and specific thrust loss are reduced by by 5.5% and 6.8%, respectively.

It is important to assess the performance of the design vanes across a range of angles of attack, even though the optimization was performed at $\alpha = 10°$. The deflection angle, thrust loss, and specific thrust loss were computed for α ranging from 0° to 15°. Figure 11 plots thrust loss versus angle of attack α and versus deflection angle ϵ. It is seen that the design vanes give consistently better performance than the NACA0012 vanes. The benefits are in fact accentuated at angles of attack (and deflection angles) larger than the design point. At ϵ=1.8°, the optimization reduces thrust loss by 15.0% for the 3-mm vane and 10.22% for the 4-mm vane. Analogous plots for the specific thrust loss are shown in Fig. 12. The significance of the specific-thrust results is that mass-flow-rate losses can be simply reversed by slight enlargement of the fan exit area. At

ϵ=1.8°, the optimization reduces specific-thrust loss by 22.5% for the 3-mm vane and 12.0% for the 4-mm vane.

Finally we examine an arrangement with two pairs of vanes mounted at 90° and 150° azimuth angles and inclined at $\alpha = 10.0°$. Figure 13 shows the comparison of pressure coefficient between the optimized and NACA0012 vanes at their mid-span. Although there are some interactions between the two pairs vanes, the nearly-constant pressure distribution on the upper surface of the optimized vanes is preserved. This indicates that results from the optimization process for a single pair of vanes are applicable to two pairs of vanes, provided that the two pairs are not too close to each other.

IV. Conclusions

An adjoint method is applied for the aerodynamic shape optimization of deflector vanes installed in the fan nozzle of a turbofan engine. The vanes deflect fan flow in the general downward direction for the purpose of suppressing noise emitted by the core stream. The specific application of this study is for a supersonic turbofan engines with bypass ratio 2.7. The cost function used in the optimization involves the entropy generated by the vanes and a penalty for deviating from a target deflection angle. The initial vane airfoil is the NACA0012 with 12% thickness. The vane airfoil arising from the optimization is thicker, with larger leading edge radius and with nearly constant pressure over most of the upper surface. The pressure bubble at the leading edge completely removed. The reduction in the adverse pressure gradient compared to the NACA0012 vane mitigates the possibility of a strong shock wave forming over the upper surface. Aerodynamic improvements are noted for entire range of angles of attack considered in this study. For a fixed flow deflection angle, the optimal airfoil is up to 22.5% more efficient in terms of specific thrust loss compared to the NACA0012. Importantly, the thicker airfoil arising from the optimization may be advantageous for structural reasons.

Acknowledgements

The support by NASA Cooperative Agreement NNX07AC62A (monitored by Dr. K.B.M.Q. Zaman) is gratefully acknowledged.

References

[1] Papamoschou, D., "New Method for jet Noise Reduction in Turbofan Engines," *AIAA Journal*, Vol. 42, No. 11, 2004, pp. 2245–2253.

[2] Papamoschou, D., "Fan Flow Deflection in Simulated Turbofan Exhaust," *AIAA Journal*, Vol. 44, No. 12, 2006, pp. 3088–3097.

[3] Papamoschou, D. and Nielsen, P., "Fan Flow Deflection for Supersonic Turbofan Engines," AIAA 2008-0039, Janurary 2008.

[4] Nielsen, P. and Papamoschou, D., "Optimization of Fan Flow Deflection for Supersonic Turbofan Engines," AIAA 2008-3061, May 2008.

[5] Xiong, J., Liu, F., and Papamoschou, D., "Computation of the Flow of a Dual-Stream Jet with Fan-Flow Deflectors for Noise Reduction," AIAA 2009-3254, June 2009.

[6] Jameson, A., "Aerodynmaic Design via Control Theory," *J. Sci. Comput.*, Vol. 3, No. 3, 1988, pp. 233–260.

[7] Jameson, A., Pierce, N., and Martinelli, L., "Optimum Aerodynmaic Design Using the Navier Stokes Equation," *Theor. Comput. Fluid Dyn.*, , No. 10, 1998, pp. 213–237.

[8] Jameson, A., "Aerodynmaic Shape Optimization using the adjoint method," Lectures at von karman institute, Feb. 2003.

[9] Saiyed, N. H., Mikkelson, K. L., and Bridges, J. E., "Acoustics and Thrust of Separate-Flow High-Bypass-Ratio Engines," *AIAA Journal*, Vol. 41, No. 3, 2003, pp. 372–378.

[10] Luo, J., Xiong, J., Liu, F., and McBean, I., "Three-dimensional Aerodynamic Design Optimization of a Turbine Blade by Using an Adjoint Method," To appear in Journal of Turbomachinery, 2010.

[11] Liu, F. and Zheng, X., "A Strongly Coupled Time-Marching Method for Solving the Navier-Stokes and k-ω Turbulence Model Equations with Multigrid," *Journal of Computational Physics*, Vol. 128, No. 10, 1996, pp. 257–284.

[12] Xiong, J., Nielsen, P., Liu, F., and Papamoschou, D., "Computational Validation of Fan Flow Deflection for Supersonic Turbofan Engines," AIAA 2009-3254, May 2009.

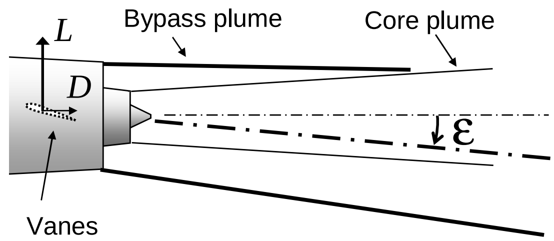

Figure 1. General concept of fan flow deflection.

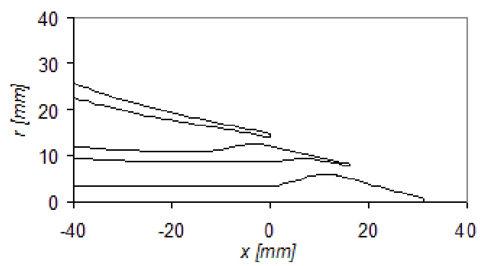

Figure 2. Coordinates of the bypass ratio BPR = 2.7 nozzle. Fan pressure ratio =2.25.

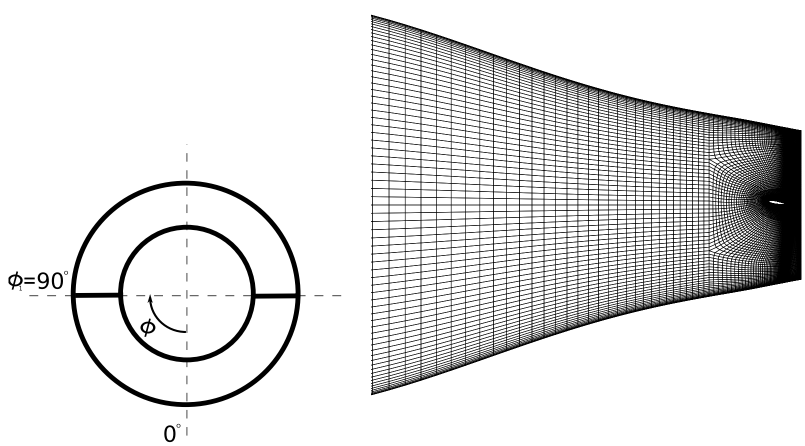

(a) 2Va configuration (b) Computational mesh

Figure 3. Cross-section illustration of 2-vane configuration and computational mesh.

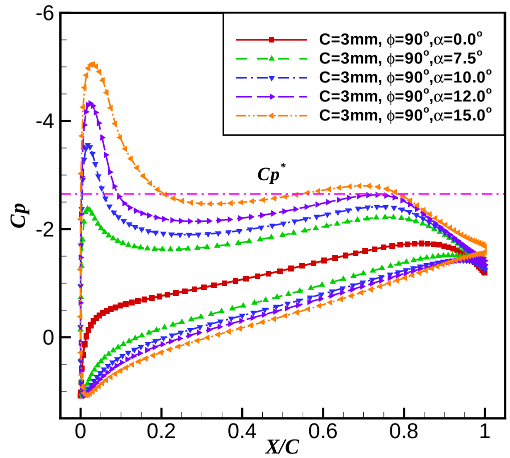

Figure 4. Pressure coefficient distribution of 3-mm chord vanes.

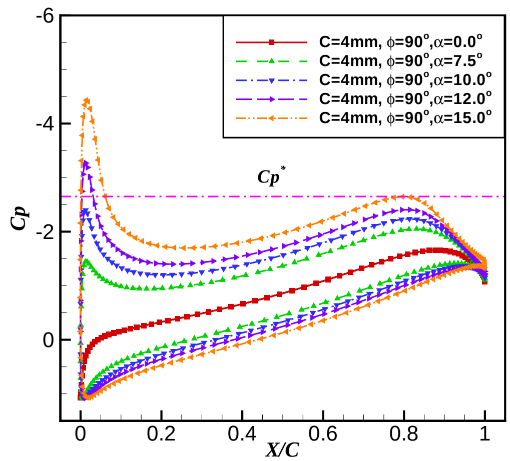

Figure 5. Pressure coefficient distribution of 4-mm chord vanes.

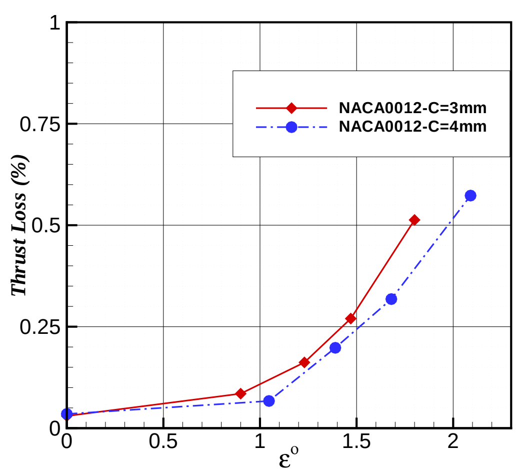

Figure 6. Thrust loss against deflection angle for single pair of NACA0012 vanes.

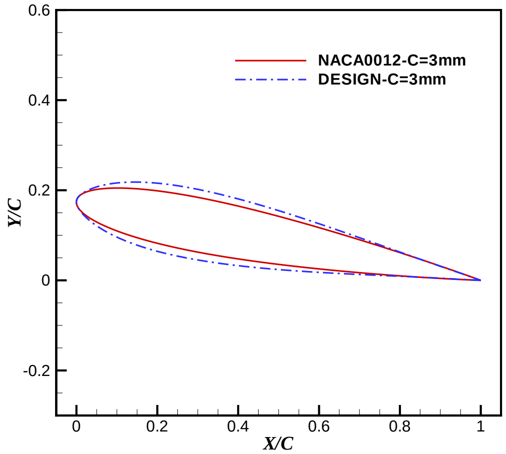

(a) Comparison of vane profile

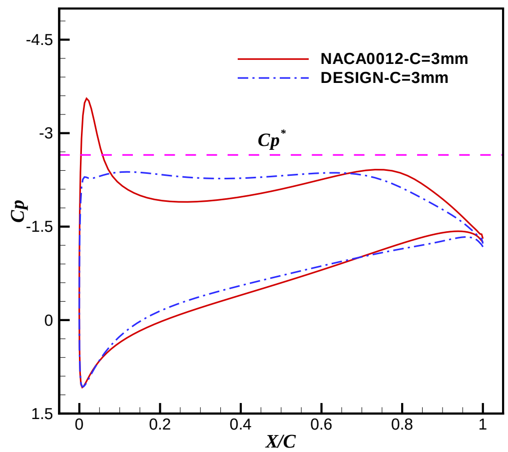

(b) Comparison of vane pressure coefficient distribution

Figure 7. Comparison of airfoil shape and pressure distribution of 3-mm vane at mid-span.

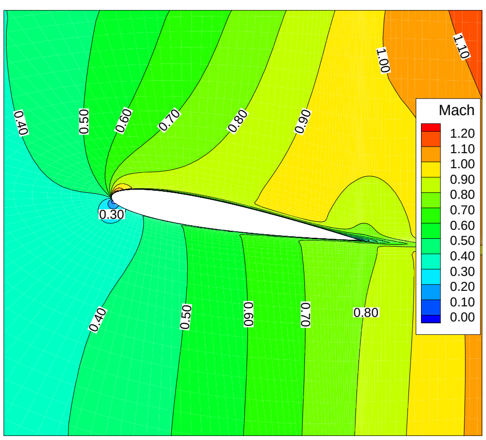

(a) NACA0012 Vane

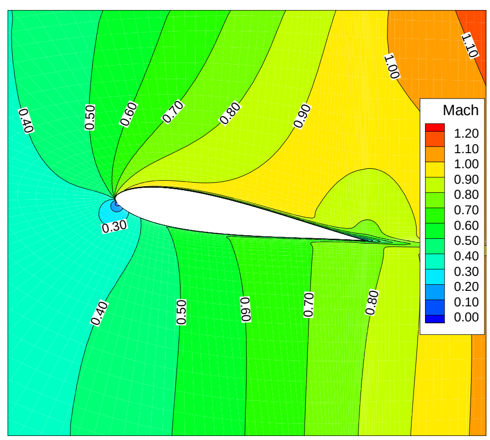

(b) Design Vane

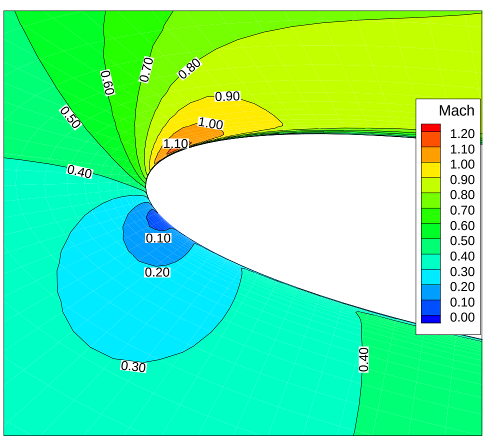

(c) NACA0012 Vane (closeup)

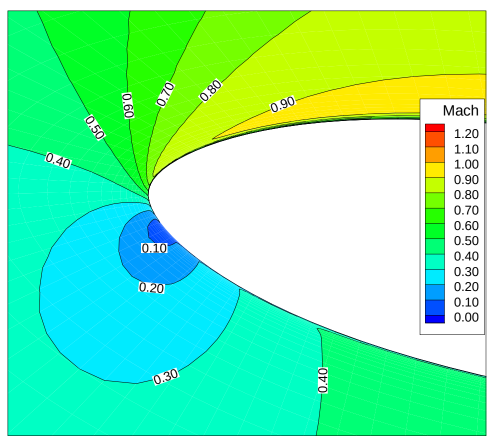

(d) Design Vane (closeup)

Figure 8. Comparison of Mach number contours of 3-mm vane at mid-span.

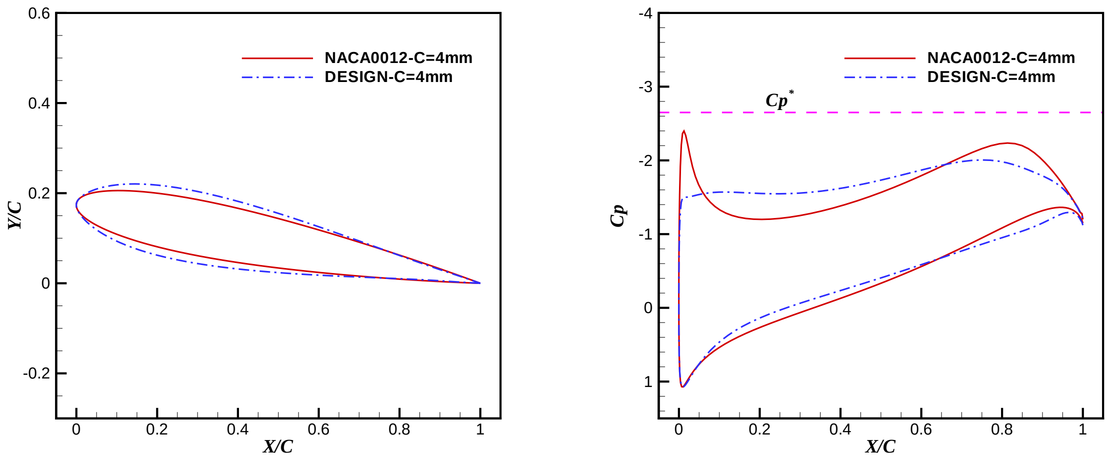

(a) Comparison of vane profile

(b) Comparison of vane pressure coefficient distribution

Figure 9. Comparison of airfoil shape and pressure distribution of 4-mm vane at mid-span.

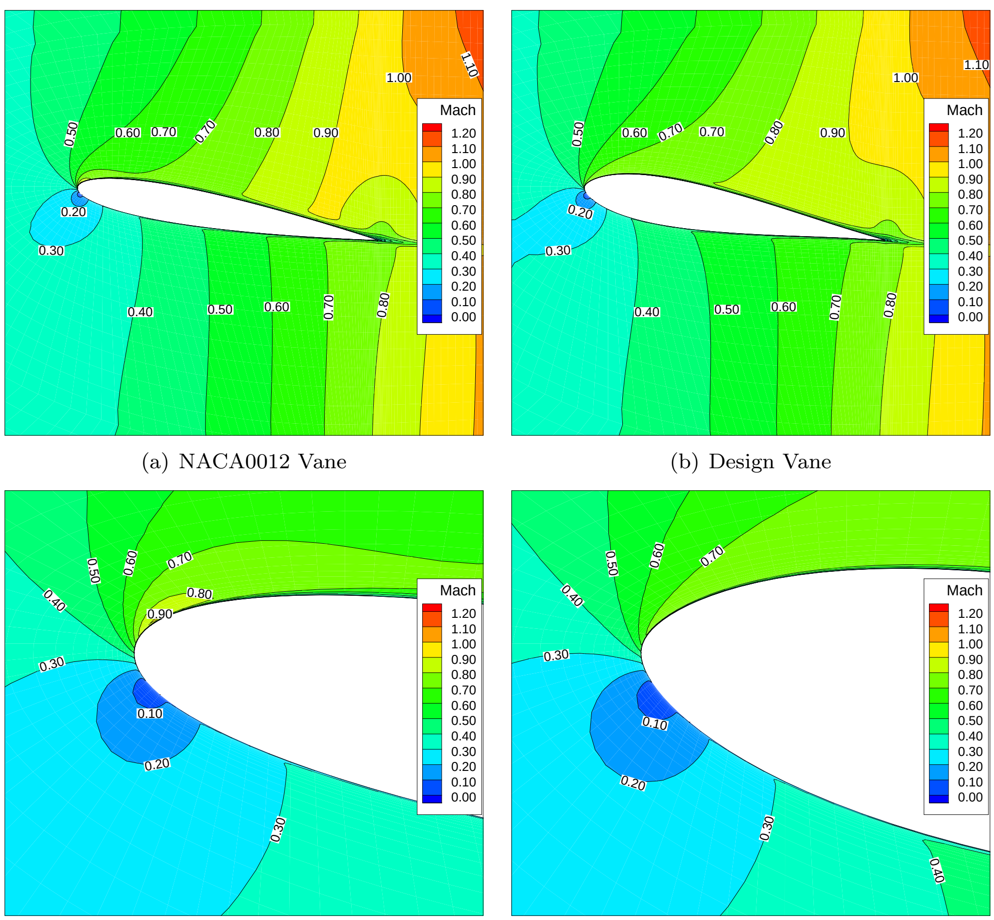

(a) NACA0012 Vane

(b) Design Vane

(c) NACA0012 Vane (closeup)

(d) Design Vane (closeup)

Figure 10. Mach number contours of 4-mm vane at mid-span.

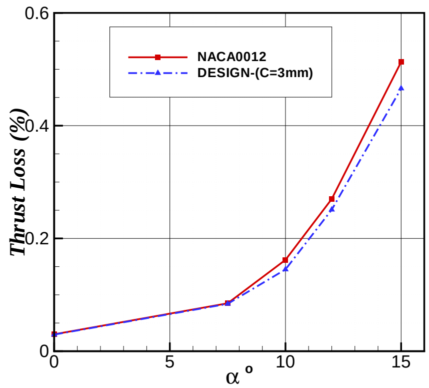

(a) Thrust loss versus angle of attack for 3mm vanes

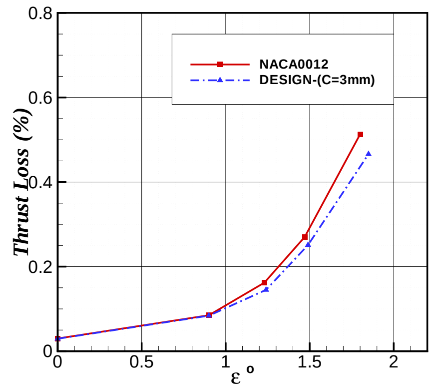

(b) Thrust loss versus deflection angle for 3mm vanes

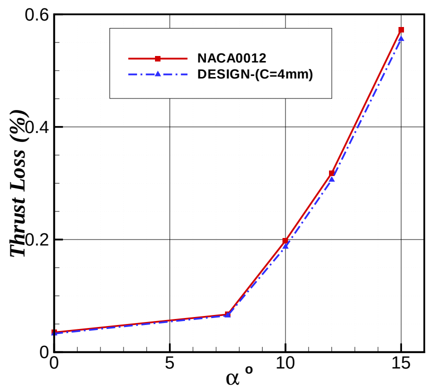

(c) Thrust loss versus angle of attack for 4mm vanes

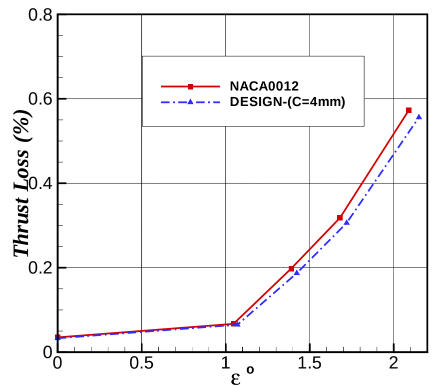

(d) Thrust loss versus deflection angle for 4mm vanes

Figure 11. Percent thrust loss versus angle of attack and versus deflection angle.

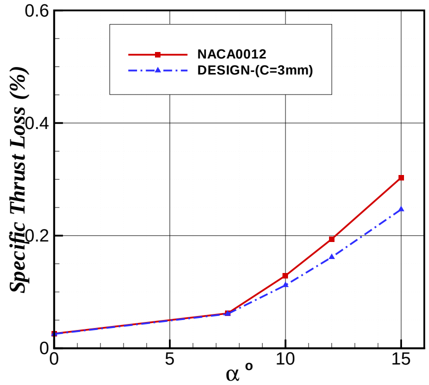

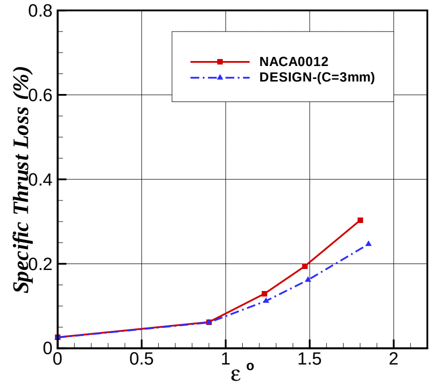

(a) Specific thrust loss versus angle of attack for 3mm vanes

(b) Specific thrust loss versus deflection angle for 3mm vanes

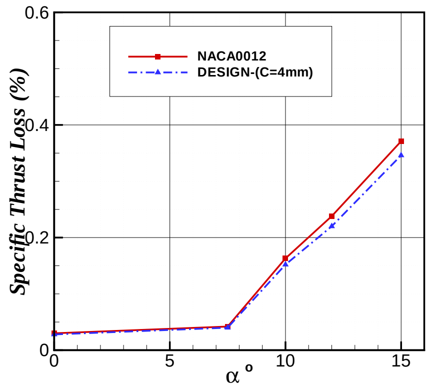

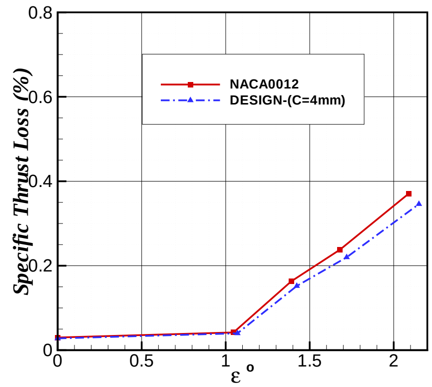

(c) Specific thrust loss versus angle of attack for 4mm vanes

(d) Specific thrust loss versus deflection angle for 4mm vanes

Figure 12. Percent specific thrust loss versus angle of attack and versus deflection angle.

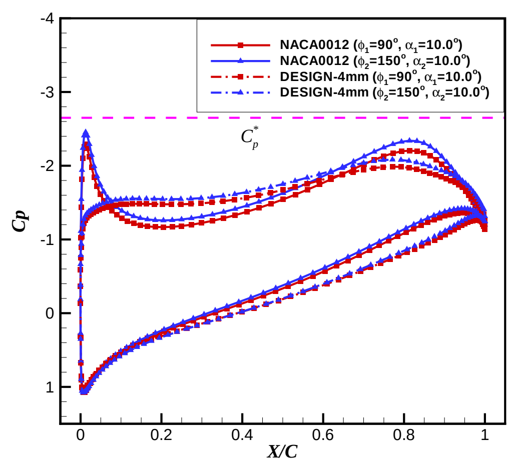

Figure 13. Pressure coefficient at mid-span of airfoils in an arrangement of two pairs of vanes.